Solar Phys (2014) 289:4711–4726
DOI 10.1007/s11207-014-0595-6

Total Solar Irradiance Monitor for Chinese FY-3A and FY-3B Satellites – Instrument Design

Wei Fang · Hongrui Wang · Huiduan Li · Yupeng Wang

Received: 27 November 2013 / Accepted: 1 September 2014 / Published online: 30 October 2014

Abstract The *Total Solar Irradiance Monitor* (TSIM) instrument is designed to perform daily observations of total solar irradiance (TSI) in space on the Chinese FY-3A and FY-3B satellites. Three absolute radiometers are constructed for the TSIM to achieve measurements with traceability to SI with an absolute accuracy better than 550 ppm. The absolute radiometers are implemented based on the principle of electrical substitution. The design of the absolute radiometers and their electrical system, operation modes in space, and uncertainty evaluation are described. A method for calculating the electrical power in the observation and reference phases is proposed to maintain the primary cavity at a nearly constant temperature.

Keywords Solar irradiance · Solar radiometry

1. Introduction

Total solar irradiance (TSI) has been identified as an important factor influencing the Earth's climate system. Continuous measurements of the TSI have been conducted on various space platforms since November 1978 (Fox *et al.*, 2011; Frohlich, 2011), including the *Earth Radiation Budget* (ERB) experiment on the NIMBUS-7 spacecraft (Hoyt

W. Fang · H. Wang (✉) · Y. Wang
Department of Space Optics 1st, Changchun Institute of Optics, Fine Mechanics and Physics, Dong Nanhu Road 3888, Changchun 130033, China
e-mail: wanghongrui03@sina.com

W. Fang
e-mail: tsim01@sina.com

Y. Wang
e-mail: wangyupeng@ciomp.ac.cn

H. Li
Department of Chemistry and Life Science, Chuxiong Normal University, Lu Cheng Nan Road 546, Chuxiong 675000, China
e-mail: lhd08@cxtc.edu.cn

et al., 1992), the *Active Cavity Radiometer Irradiance Monitor* (ACRIM I) experiment on the *Solar Maximum Mission* (SMM) (Wilson, 1997), the ACRIM II experiment on the *Upper Atmosphere Research Satellite* (UARS), the *Variability of Solar Irradiance and Gravity Oscillations* (VIRGO) experiment on the *Solar and Heliospheric Observatory* (SOHO) (Frohlich *et al.*, 1997), and the *Total Irradiance Monitor* (TIM) experiment on the *Solar Radiation and Climate Experiment* (SORCE) (Kopp and Lawrence, 2005; Kopp, Heuerman, and Lawrence, 2005).

The FY-3 TSI database has been constructed from the data obtained since 2008 with the *Total Solar Irradiance Monitor* (TSIM) on the Feng Yun-3 series satellites (FY-3; Feng means wind in Chinese, Yun means cloud in Chinese; Wang and Wang, 2012). The FY-3 series satellites are Chinese meteorological polar-orbit satellites (Yang *et al.*, 2012). FY-3A, the first satellite of the series, was launched on 27 May 2008. FY-3B, the second satellite of the series, was launched on 5 November 2010. TSIM/FY-3A recorded the TSI daily from June 2008 to December 2011. The FY-3 TSI database is further extended by overlapping observations by TSIM/FY-3B from November 2010 to the present.

The TSIM/FY3-B instrument has almost the same design as TSIM/FY-3A, except for some software improvements for the onboard components. The TSIM is installed on the leading surface of the satellite, with its opening parallel to the flying direction of the satellite. Neither FY-3A nor FY-3B make the TSIM point accurately toward the Sun. In addition, the TSIM has no solar tracking device (Wang, Wang, and Fang, 2011). Thus, the Sun is only observed when the satellite leaves the Earth's shadow near the terrestrial North Pole and sunlight sweeps the TSIM field of view (Fang *et al.*, 2002).

The TSIM was calibrated to World Radiometric Reference through ground-based comparison experiments (Wang, Li, and Fang, 2014). Absolute radiometers SIAR-1a and SIAR-2c were used as transfer standard, which had been calibrated to World Radiometric Reference by World Standard Group TSI instruments in the tenth International Pyrheliometer Comparison (IPC-X), 2005.

2. Design

The instrument overview of the TSIM is shown in Figures 1 and 2. The electronics of the TSIM is shown in Figure 3. The instrument consists of the three absolute radiometers AR1, AR2, and AR3, as illustrated in Figure 2. The three radiometers and an amplifier for the temperature signal are integrated into the instrument, while other electrical systems for the TSIM are implemented in the electronics package. Some parameters of the TSIM are presented in Table 1.

The three absolute radiometers take independent measurements or simultaneous measurement of the TSI on command. The radiometers AR1 and AR2 are designed for regular observation of the TSI, while the radiometer AR3 is designed for occasional observation to investigate the degradation of AR1 and AR2. The three radiometers are aligned with different inclinations with respect to the mounting surface of the TSIM to increase their fields of view (Liebetraut *et al.*, 2013; Memarian and Eleftheriades, 2013; Witte *et al.*, 2014). The angle between the optical axis of each radiometer and the satellite X-axis is given in Table 1.

2.1. Absolute Radiometer

Each absolute radiometer is constructed based on the principle of electrical substitution (Wilson, 1979). The radiometer has two inverted cone cavities, as shown in Figure 4. One

Figure 1 An overview of TSIM/FY-3B. It consists of the three absolute radiometers AR1, AR2, and AR3.

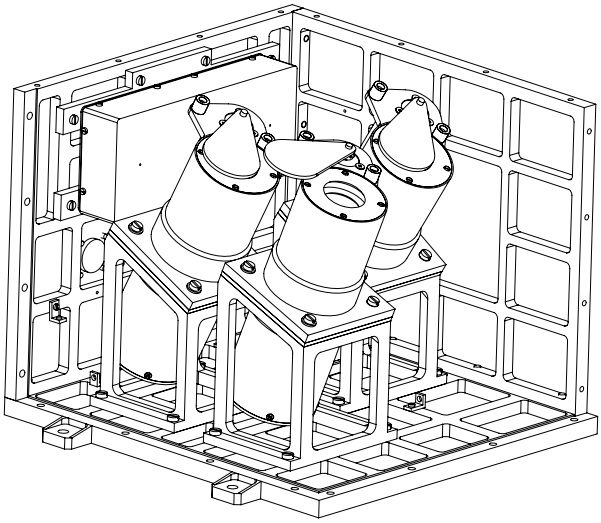

Figure 2 Schematic drawing of the instrument. The three absolute radiometers and an amplifier for the temperature signal are integrated into the instrument.

is the primary cavity, the other the reference cavity for compensation. The two cavities are installed together in a single aluminum cylinder. The cylinder serves as a heat sink to stabilize the thermal system of the radiometer. A precision aperture is located in front of the primary cavity. The precision aperture was fabricated carefully, and its area has been measured by repeated experiments. A shutter unit and an aperture for view limiting are located at the top of the heat sink to control sunlight input to the primary cavity (Booth, 2014; Girshovitz and Shaked, 2014). Several apertures are mounted between the precision aperture and the view-limiting aperture to prevent stray light from entering the primary cavity.

The primary cavity is a silver cone cavity with thin walls. The thickness of the cone wall is 0.06 mm. The internal surface of the primary cavity is coated with a thin layer of absorptive black paint. The reflectivity of this paint is nearly uniform in the wavelength range of the instrument. The effective absorption coefficient of the cone cavity is 0.9997. The

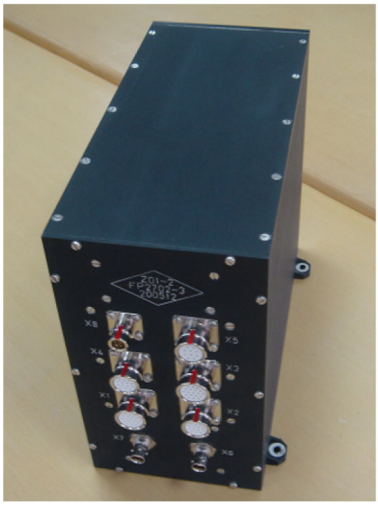

Figure 3 The electronics package of TSIM/FY-3B. It includes among others units of A/D conversion, communication with the satellite, and precision voltage reference.

Table 1 Parameters for TSIM/FY-3B.

Wavelength range	0.2 μm – 50 μm
Field of view	26.6°
Range of irradiance measurement	100 W m^{-2} – 1400 W m^{-2}
Measurement sensitivity	0.2 W m^{-2}
Relative uncertainty	< 550 ppm
Mass of the instrument	8.82 kg
Mass of the electronics	5.91 kg
Power consumption of the instrument	3.68 W
Power consumption of the electronics	5.46 W
Mechanical size of the instrument	260.12 mm × 240.15 mm × 210.03 mm
Mechanical size of the electronics	265.64 mm × 124.31 mm × 224.03 mm
Angle between the AR1 optical axis and the satellite X-axis	21.97°
Angle between the AR2 optical axis and the satellite X-axis	26.95°
Angle between AR3's optical axis and the satellite X-axis	32.02°

heating wires are embedded into the thin walls of the primary cavity using electroplating. Nearly all the power produced by the heating wires is absorbed by the cone cavity with little heat loss, thanks to this method.

A ring with a radius of 13 mm, surrounded by 180 pairs of thermocouples, is laid at the opening bottom of the primary cavity. The reference cavity also has a ring of thermocouples. The hot junctions of the thermocouples are connected to the primary cavity, while the cold junctions are connected to the heat sink. The ring of thermocouples is used as a passive temperature sensor to detect the temperature difference between the primary cavity and the heat sink. The reference cavity receives no sunlight and is not electrically heated either. The ring of thermocouples of the reference cavity is connected in series to the ring of thermocouples of the primary cavity. The purpose of the series connection is to compensate for any varia-

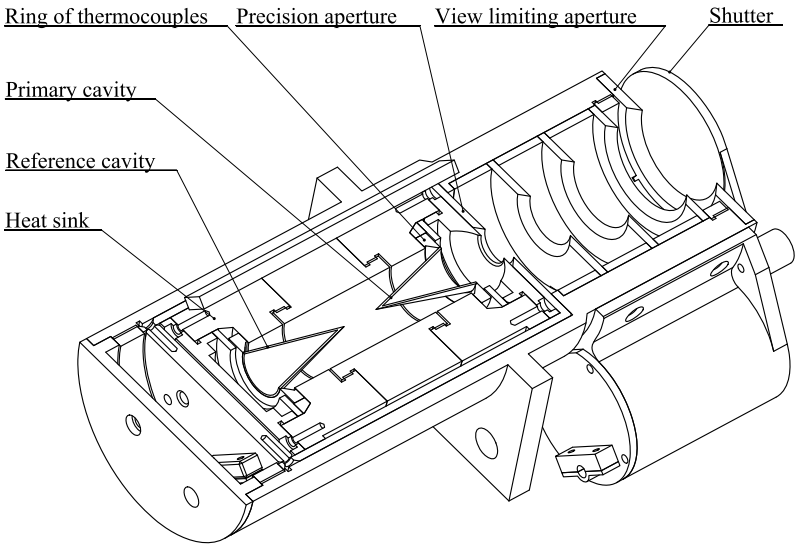

Figure 4 Schematic drawing of the absolute radiometer.

tion in the output from the ring of thermocouples that is caused by a temperature change in the heat sink.

2.2. Electronics

A block diagram of the TSIM electronics is given in Figure 5. The electronics package includes an amplifier for the temperature signal, an A/D converter for the temperature signal, three D/A converters for electrical substitution, three driving circuits for the shutters, three driving circuits for heating the primary cavity, a communication unit with the satellite, a precision voltage reference, a remote measurement unit, a micro-controller unit, and others. The three radiometers have the same circuits as the A/D conversion, communication with the satellite, precision voltage reference, and the micro-controller. Each radiometer has independent circuits for D/A conversion, shutter driver, and heating driver. A Zener-based integrated circuit LM199H was selected as the precision voltage reference for electrical substitution. The voltage applied to the primary cavity for heating is always calibrated by LM199H. This has excellent temperature stability over the operating temperature range of the instrument, namely -55 °C to 125 °C and for different operating current conditions; its typical long-term stability is 8 ppm/$\sqrt{\text{kH}}$. Changes in voltage with temperature are almost eliminated by integrating the output from an active Zener diode on the monolithic substrate of LM199H.

When sunlight is fed to the radiometer, the temperature of the primary cavity is measured by the temperature sensor, that is, by the ring of thermocouples. The temperature of the primary cavity is further converted into a digital signal by a 16 bit A/D converter. The digital temperature signal is then sent to the micro-controller. The power of the incoming sunlight is estimated by the micro-controller, and then an equivalent electrical heating power is determined. The estimation method is described in detail in Section 4. Conversely, when the shutter is closed, the power for electrical substitution is calculated and a proper voltage is generated by the D/A converter. The heating voltage is applied to the heating wires

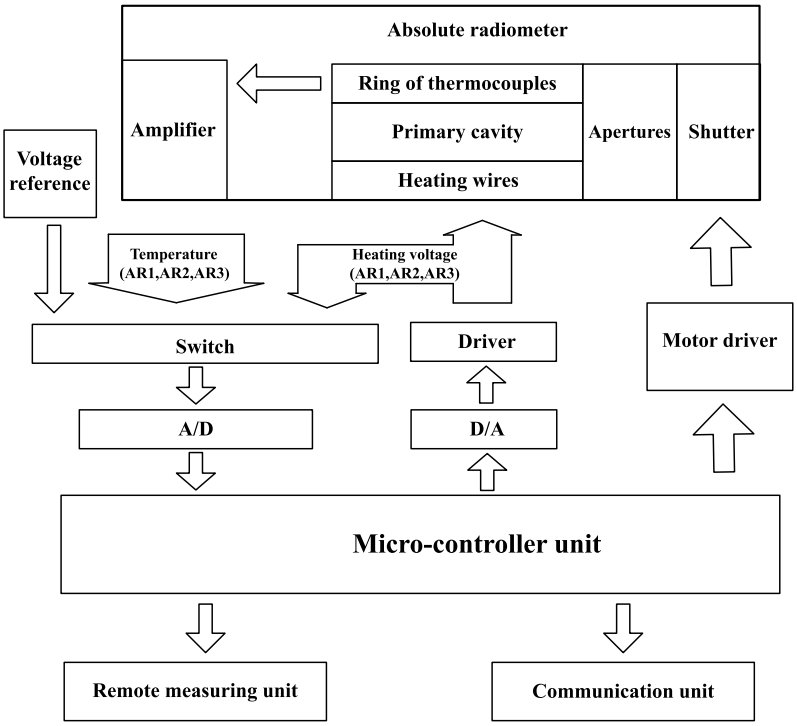

Figure 5 A block diagram of the TSIM electronics. Most of the TSIM electronics is implemented in this electronics package.

through amplification in the driving circuits for the heating of the primary cavity. Specific experiment data are collected and stored by the micro-controller as remote sensing data. The remote sensing data are then sent to the data management system of the satellite through the communication unit.

2.3. Measurement Sequence

When no operation is performed, as described in Section 3, a constant electrical power P_{m} is always applied to the primary cavity to keep it at an almost constant temperature T_{c} in the orbit.

The value of the TSI is calibrated once in two subsequent phases: the observation phase and the reference phase (Wilson, 1979). In the observation phase, the shutter is open and sunlight is allowed to fall onto the primary cavity. Less electrical power is needed as a result of the absorbed energy of the incoming sunlight. In the reference phase, the shutter is closed and more electrical power is applied to keep the primary cavity at an almost constant temperature. Because the applied electrical power can be measured precisely, an accurate measure of the TSI is available (Wilson, 1979; Kopp and Lawrence, 2005; Mekaoui *et al.*, 2010).

In the observation phase, a voltage u_{eo} is applied to the primary cavity. After the temperature of the primary cavity stabilizes at a constant value T_{o}, the absorbed radiant power P_{s}

is given by

$$P_s = E \cdot A \cdot \alpha, \tag{1}$$

where E is the solar irradiance, A is the area of the precision aperture, and α is the effective absorption coefficient of the primary cavity.

In the reference phase, voltage u_{er} is applied to the primary cavity to stabilize the temperature of the primary cavity again at T_o. When the stable temperature of the primary cavity in the reference phase is the same as the stable temperature in the observation phase, the relationship

$$P_s + \frac{u_{eo}^2}{R} = \frac{u_{er}^2}{R} \tag{2}$$

holds, where R is the resistance of the heating wires for the primary cavity.

When the TSIM works in the operation modes that are introduced in Section 3, the temperature of the primary cavity is sampled every 5 s by the 16 bit A/D converter.

3. Operation Modes

The TSIM works continuously in the orbit, and the value of the TSI is observed once every orbit by the radiometers. The radiometers have three operation modes: a test mode, a solar observing mode, and a background mode.

The temperature of the primary cavity presented in this section is given as a binary number from the A/D converter in units of the least significant bit (LSB) of its output. The temperature of the primary cavity is not transformed into kelvin for simplicity.

3.1. Test Mode

When the TSIM needs to be checked in the orbit, such as in the power-on sequence of the instrument, the TSIM enters the test mode. The electrical power as illustrated in Figure 6 is applied to the primary cavity. The temperature record of the primary cavity in the test mode is shown in Figure 7. The sequence of procedures followed during the test mode is listed below:

1) Close the shutter of the radiometer, apply a low power P_L to the primary cavity for 6 min, and the temperature of the primary cavity stabilizes at a temperature T_L.

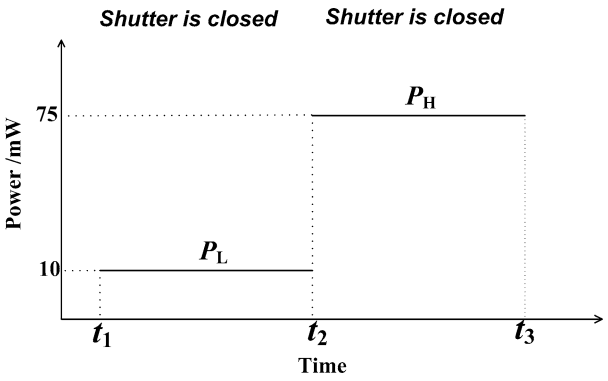

Figure 6 Electrical heating power profile of the test mode.

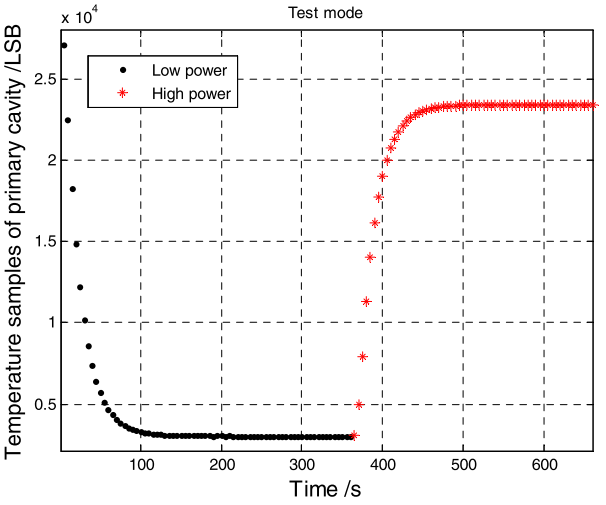

Figure 7 Temperature response of the primary cavity in the test mode. The data were obtained by TSIM/FY-3B in space at 1:02 UT, 11 November 2010. This is the first remote-sensing data set obtained by TSIM/FY-3B. The temperature of the primary cavity is given in units of the LSB of the A/D converter output.

2) Keep the shutter of the radiometer closed, apply a high power P_{H} to the primary cavity for 5 min, and the temperature of the primary cavity stabilizes at a temperature T_{H}. The value of P_{H} is equal to the maintaining electrical power P_{m}.

3) Compute the sensitivity of the primary cavity of the radiometer s_{pt} by

$$s_{\mathrm{pt}} = \frac{P_{\mathrm{H}} - P_{\mathrm{L}}}{T_{\mathrm{H}} - T_{\mathrm{L}}}. \tag{3}$$

The sensitivity indicates how much electrical power is required to increase the temperature of the primary cavity by a specified amount. The sensitivity s_{pt} is shown in Figure 8 in units of W/LSB.

4) Produce a remote-sensing data set of the radiometer in the test mode.

3.2. Solar Mode

When sunlight is visible within the TSM field of view, the instrument enters the solar mode. The electrical power as illustrated in Figure 9 is applied to the primary cavity. The temperature response of the primary cavity in the solar mode is shown in Figure 10. The sequence of procedures of the solar observing mode is listed below:

1) Open the shutter of the radiometer and apply a power P_{soe} to the primary cavity for 6 min. How to determine the power P_{soe} is explained in detail in Section 4. The temperature of the primary cavity stabilizes at temperature T_{so}.

2) Close the shutter of the radiometer for 5 min and apply a power P_{sre} to the primary cavity to stabilize the temperature again at T_{so}. When the temperature of the primary cavity stabilizes at the end of the reference phase, the value of E (TSI) is obtained from Equations (1) and (2) as

$$E = \frac{P_{\mathrm{sre}} - P_{\mathrm{soe}}}{A \cdot \alpha}. \tag{4}$$

3) Produce a remote-sensing data set of the radiometer in the solar mode.

When a remote-sensing data set is produced in the solar mode, the shutter of the radiometer is opened to detect the sunlight. If the temperature of the primary cavity exceeds a

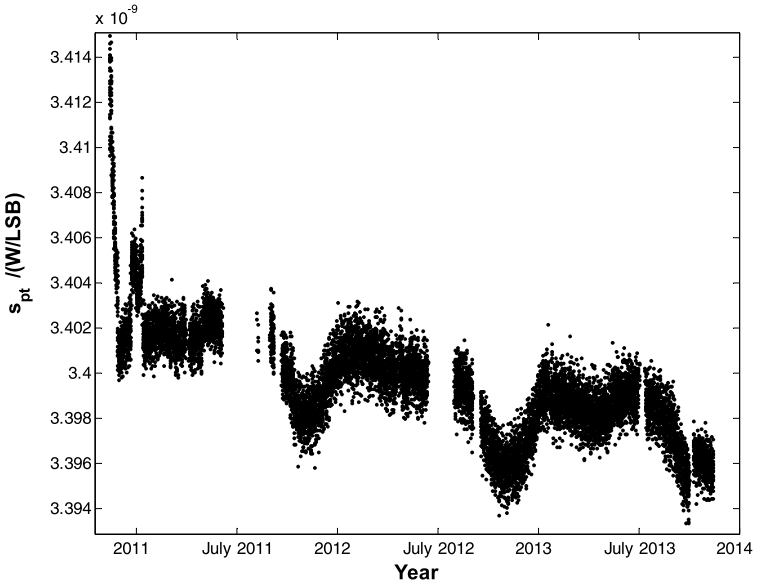

Figure 8 Sensitivity (s_{pt}) of the radiometer AR2 in TSIM/FY-3B from 11 November 2010 to 10 November 2013. Some data gaps occured (*e.g.* in July 2011) because the instrument occasionally stopped working as a result of electronics problems.

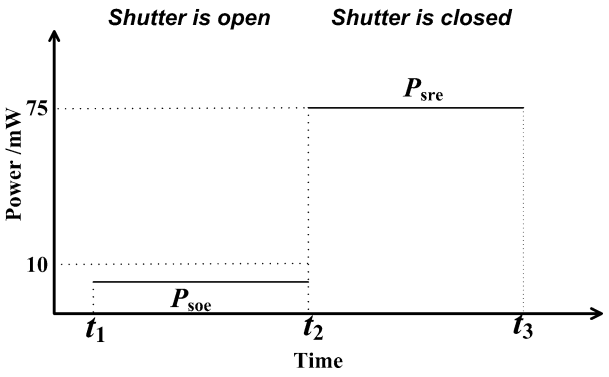

Figure 9 Electrical heating power profile of the solar mode in the observation and the reference phases.

given value, it means that sunlight enters the field of view of the radiometer again, and the radiometer will start the next TSI measurement.

3.3. Background Mode

When the shutter of the radiometer is open in the solar mode, the radiometer emits radiative power to space. The radiative power exchange between the cosmic background and the radiometer is given by

$$\varphi_{\mathrm{rb}} = \int_{S_{\mathrm{r}}} \int_{S_{\mathrm{b}}} \frac{(L_{\mathrm{b}} - L_{\mathrm{r}}) \cos\theta_{\mathrm{b}} \cos\theta_{\mathrm{r}}}{r^2} \, \mathrm{d}S_{\mathrm{b}} \, \mathrm{d}S_{\mathrm{r}}, \tag{5}$$

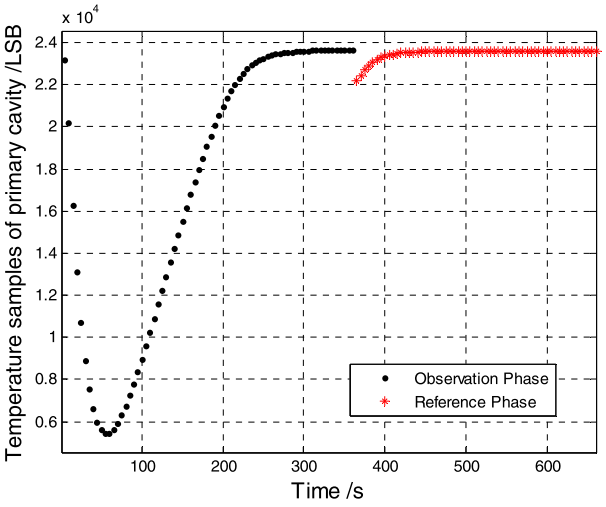

Figure 10 Temperature response of the primary cavity in the solar mode. The data were obtained by radiometer AR1 of TSIM/FY-3B in space at 1:51 UT, 11 November 2010. This was the first sunlight for TSIM/FY-3B. The temperature of the primary cavity is given in units of the LSB of the A/D converter output.

where φ_{rb} is the radiative power from the cosmic background to the primary cavity of the radiometer, L_{b} is the radiance of the cosmic background, L_{r} is the radiance of the radiometer, S_{r} is the surface of the precision aperture of the radiometer, S_{b} is the surface of cosmic background (the two surfaces are joined by a light ray of length r), θ_{b} is the angle between the light ray and the normal to the surface S_{b}, and θ_{r} is the angle between the light ray and the normal to the surface S_{r}. From Plank's law and Equation (5), we obtain

$$\varphi_{\mathrm{rb}} = \frac{\sigma\left(T_{\mathrm{b}}^4 - T_{\mathrm{m}}^4\right)}{\pi} \int_{S_r} \cos\theta_{\mathrm{r}}\,\mathrm{d}S_{\mathrm{r}} \int_0^{\omega} 2\pi \cos\theta_{\mathrm{b}} \sin\theta_{\mathrm{b}}\,\mathrm{d}\theta_{\mathrm{b}}, \tag{6}$$

where σ is the Stefan–Boltzmann constant ($\sigma = 5.670 \times 10^{-8}\ \mathrm{W\,m^{-2}\,K^{-4}}$), T_{b} is the temperature of the cosmic background ($T_{\mathrm{b}} = 2.72548$ K), T_{m} is the temperature of the primary cavity, and 2ω is the field of view of the radiometer.

For a light ray leaving the primary cavity, we can set

$$\theta_{\mathrm{r}} = 0. \tag{7}$$

Then, Equation (6) becomes

$$\varphi_{\mathrm{rb}} = \sigma A\left(T_{\mathrm{b}}^4 - T_{\mathrm{m}}^4\right)\sin^2\omega, \tag{8}$$

from which follows

$$I_{\mathrm{rb}} = \sigma\left(T_{\mathrm{b}}^4 - T_{\mathrm{m}}^4\right)\sin^2\omega, \tag{9}$$

where I_{rb} is the irradiance from the cosmic background to the radiometer.

For the TSIM, $T_{\mathrm{m}} = 300$ K, $\omega = 13.3°$, and we obtain

$$I_{\mathrm{rb}} = \sigma\left(T_{\mathrm{b}}^4 - T_{\mathrm{m}}^4\right)\sin^2\omega = -24.3059\ \mathrm{W\,m^{-2}}. \tag{10}$$

Here the irradiance I_{rb} is measured in the background mode for the correction of the TSI data.

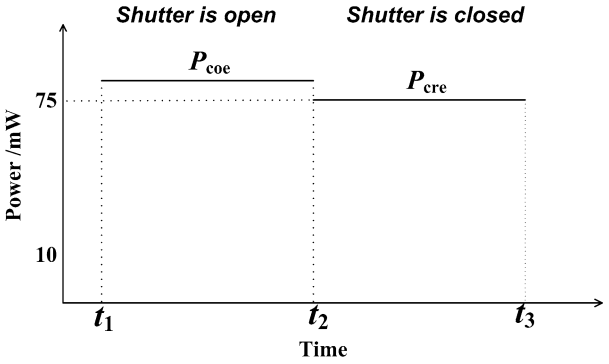

Figure 11 Electrical heating power profile of the background mode in the observation and the reference phases.

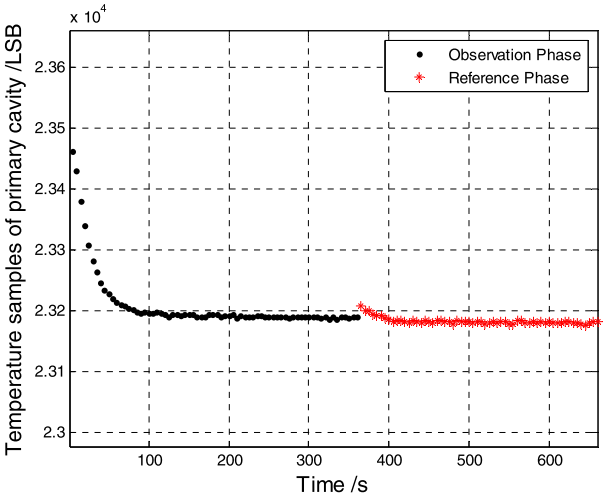

Figure 12 Temperature response of the primary cavity in the background mode. The data were obtained by radiometer AR1 of TSIM/FY-3B in space at 2:08 UT, 11 November 2010. This was the first measurement of cosmic background by TSIM/FY-3B. The temperature of the primary cavity is given in units of the LSB of the A/D converter output.

The heating power profile applied to the primary cavity in the background mode is shown in Figure 11, and the temperature response of the primary cavity in the background mode is shown in Figure 12. The sequence of procedures followed during the background mode is as follows:

1) Ten minutes after the TSIM receives the information that the satellite is in the Earth shadow, the shutter of the radiometer is opened. A power P_{coe} is applied to the primary cavity for 6 min. The temperature of the primary cavity gradually decreases as a result of the radiative power from the primary cavity to the cosmic background, and finally stabilizes at T_{co}.

2) Close the shutter of the radiometer for 5 min and apply a power P_{cre} to the primary cavity to stabilize its temperature again at T_{co}.

3) Compute the radiative power from the cosmic background to the radiometer and produce a remote-sensing data set of the radiometer for the background mode.

4. Estimation of Required Electrical Power

A stable temperature of the primary cavity is helpful for quick measurements of TSI values. Our experiments have proved that when the temperature of the primary cavity varies sub-

stantially, more time is generally necessary to complete a single measurement. In addition, the measurement accuracy is influenced by the temperature variations. The primary cavity of the TSIM radiometer is always expected to be maintained at an almost constant temperature. However, the precise electrical power required in the observation phase is not known in advance. It needs to be determined consistently and carefully, especially in the solar mode. The method for estimating the required electrical power is described in this section.

When a radiometer operates in the observation phase of the solar mode, the electrical power is reduced to zero as soon as the shutter is open. The temperature of the primary cavity decreases from a constant temperature T_c. If a sufficiently long time t has elapsed in the observation phase, the temperature of the primary cavity will stabilize at T_{so}, as described in Section 3. As a function of t, the temperature of the primary cavity will vary as

$$T(t) = (T_c - T_{so})e^{-\frac{t}{\tau}} + T_{so}. \tag{11}$$

For given times t_1 and t_2 $(t_2 > t_1)$, we obtain

$$T(t_1) - T_{so} = (T_c - T_{so})e^{-\frac{t_1}{\tau}}, \tag{12}$$

$$T(t_2) - T_{so} = (T_c - T_{so})e^{-\frac{t_2}{\tau}}. \tag{13}$$

Equation (12) divided by Equation (13) gives

$$T_{so} = \frac{T(t_1) - T(t_2)e^{\frac{t_2-t_1}{\tau}}}{1 - e^{\frac{t_2-t_1}{\tau}}}. \tag{14}$$

The power of the incoming sunlight is approximated as

$$P_{sa} = \frac{T(t_1) - T(t_2)k}{1 - k} s_{pt}, \tag{15}$$

where k is given as

$$k = e^{\frac{t_2-t_1}{\tau}}. \tag{16}$$

The electrical power P_{soe} required in the observation phase of the solar mode is found as

$$P_{soe} = P_m - P_{sa}. \tag{17}$$

Likewise, the electrical power P_{sre} required in the reference phase of the solar mode is given by

$$P_{sre} = T_{so} s_{pt}. \tag{18}$$

The electrical power required in the background mode can be derived in a similar manner as discussed above.

As proved by the remote-sensing data set shown in Figures 10 and 12, the temperature of the primary cavity is maintained at a nearly constant value using the method presented in this section.

Table 2 Results of the comparison experiment for TSIM/FY-3B.

Parameters	AR1/TSIM/FY-3B	AR2 TSIM/FY-3B	AR3/ TSIM/FY-3B
Calibration factor to WRR	0.996575	0.998776	0.995835
Uncertainty (one standard deviation)	0.003101	0.003562	0.002963

5. Comparison Experiment

The traceability of TSIM/FY-3B to the World Radiometric Reference (WRR) was achieved through ground-based comparison experiments in the air, at ambient temperature and ambient pressure (Wang, Li, and Fang, 2014). No vacuum devices were used in the instrument calibration. Solar Irradiance Absolute Radiometer (SIAR) type absolute radiometers SIAR-1a and SIAR-2c were used as transfer instruments in the comparison experiments. (A similar process was also carried out for TSIM/FY-3C.) The duration of a single TSI measurement in the comparison experiment is 10 min; 5 min each for the observation phase and the reference phase (Wang, Li, and Fang, 2014). To measure the Sun together, the three instruments TSIM/FY-3B, SIAR-1a, and SIAR-2c were pointed toward the Sun simultaneously using solar tracking devices.

SIAR-1a and SIAR-2c had previously been calibrated to WRR by World Standard Group (WSG) TSI instruments at the tenth International Pyrheliometer Comparison (IPC-X) in 2005. According to this calibration, the calibration factors to WRR are 1.001928 for SIAR-1a and 1.000016 for SIAR-2c. The calibration factors of the TSIM in the comparison experiments are presented in Table 2.

6. Evaluation of Measurement Uncertainties

The uncertainty in TSI measured with each absolute radiometer in the TSIM is modeled from Equation (4) as follows:

$$E = f(u_{\mathrm{er}}, u_{\mathrm{eo}}, R, A, \alpha) = \frac{u_{\mathrm{er}}^2 - u_{\mathrm{eo}}^2}{R \cdot A \cdot \alpha}, \tag{19}$$

where u_{eo} and u_{er} are the heating voltages in the observation and the reference phases (see Equation (2)). The combined standard uncertainty in E is

$$\begin{aligned} u_{\mathrm{c}}^2(E) &= \left(\frac{\partial f}{\partial u_{\mathrm{er}}}\right)^2 u^2(u_{\mathrm{er}}) + \left(\frac{\partial f}{\partial u_{\mathrm{eo}}}\right)^2 u^2(u_{\mathrm{eo}}) \\ &\quad + \left(\frac{\partial f}{\partial R}\right)^2 u^2(R) + \left(\frac{\partial f}{\partial A}\right)^2 u^2(A) + \left(\frac{\partial f}{\partial \alpha}\right)^2 u^2(\alpha) \\ &= 4\left(\frac{u_{\mathrm{er}}}{R \cdot A \cdot \alpha}\right)^2 u^2(u_{\mathrm{er}}) + 4\left(\frac{u_{\mathrm{eo}}}{R \cdot A \cdot \alpha}\right)^2 u^2(u_{\mathrm{eo}}) + \left(\frac{u_{\mathrm{eo}}^2 - u_{\mathrm{er}}^2}{A \cdot \alpha \cdot R^2}\right)^2 u^2(R) \\ &\quad + \left(\frac{u_{\mathrm{eo}}^2 - u_{\mathrm{er}}^2}{R \cdot \alpha \cdot A^2}\right)^2 u^2(A) + \left(\frac{u_{\mathrm{eo}}^2 - u_{\mathrm{er}}^2}{R \cdot A \cdot \alpha^2}\right)^2 u^2(\alpha). \end{aligned} \tag{20}$$

Table 3 Uncertainties in the absolute radiometers AR1 and TSIM/FY-3B.

Parameter	Value	Relative uncertainty	Absolute uncertainty
u_{er}	7.96717 V	168 ppm	1.33509×10^{-3} V
u_{eo}	2.90940 V	285 ppm	8.28815×10^{-4} V
A	5.04793×10^{-5} m^2	290 ppm	1.46544×10^{-8} m^2
R	846.510 Ω	14 ppm	0.012232 Ω
α	0.9997	120 ppm	1.20×10^{-4}
Irradiance E	1287.76 W m^{-2}	506 ppm	0.651728 W m^{-2}

Table 4 Uncertainties in the absolute radiometers AR2 and TSIM/FY-3B.

Parameter	Value	Relative uncertainty	Absolute uncertainty
u_{er}	8.09267 V	167 ppm	1.35202×10^{-3} V
u_{eo}	2.95446 V	282 ppm	8.33529×10^{-4} V
A	5.04290×10^{-5} m^2	290 ppm	1.46471×10^{-8} m^2
R	873.40 Ω	14 ppm	0.012253 Ω
α	0.9997	120 ppm	1.20×10^{-4}
Irradiance E	1289.13 W m^{-2}	505 ppm	0.651132 W m^{-2}

Table 5 Uncertainties in the absolute radiometers AR3 and TSIM/FY-3B.

Parameter	Value	Relative uncertainty	Absolute uncertainty
u_{er}	7.96390 V	168 ppm	1.33989×10^{-3} V
u_{eo}	2.90790 V	286 ppm	8.30986×10^{-4} V
A	5.04667×10^{-5} m^2	290 ppm	1.46525×10^{-8} m^2
R	845.85 Ω	14 ppm	0.012231 Ω
α	0.9997	120 ppm	1.20×10^{-4}
Irradiance E	1288.07 W m^{-2}	507 ppm	0.653482 W m^{-2}

The uncertainties in the parameter values of the absolute radiometers and the combined standard uncertainty in E are summarized in Tables 3, 4, and 5. Most of the uncertainties for individual parameters were obtained from independent repeated observations, while some were obtained from the manufacturer's specification, such as the datasheets of the A/D converter and the precision voltage reference.

The ground experiments for uncertainty evaluation were performed in the test mode of the TSIM as described in Section 3.1. It was found that the light resources used in the ground tests of TSIM/FY-3B, such as the laser (Rubenchik, Fedoruk, and Turitsyn, 2014), were always changing. As a result, no light sources were used in the experiments for uncertainty evaluation to investigate the real characteristics of the TSIM. In the test mode of the instrument, the heating voltages u_{er} and u_{eo} were set by the micro-controller unit of the TSIM electronic system and were repeated as often as necessary. In the solar mode, it was quite hard to repeat the heating voltages for the primary cavity because of changes in the light sources. Therefore, the radiometer performance of light-to-heat conversion could not be evaluated.

Uncertain correction terms for TSI science results, such as corrections for traceability, Sun–Earth distance, satellite velocity relative to the Sun, and solar pointing errors were neglected in this uncertainty evaluation.

7. Summary

The FY-3 TSI database has been constructed from data from the TSIM/FY-3A and TSIM/FY-3B instruments obtained from June 2008 to the present. Daily observations of the TSI with traceability to SI have been performed by the TSIM, using three absolute radiometers. The performance of the TSIM has been improved in the following points: 1) The heating wires are embedded into the walls of the primary cavity and are not wrapped on its surface, to reduce loss of heating power. 2) Radiative power exchange between the cosmic background and the absolute radiometer is measured in the background mode every orbit, and they are identified as compensation terms in the correction of TSI data. 3) To quickly perform TSI measurements, the required electrical power for the heater is estimated by calculation. This helps to maintain the primary cavity at an almost constant temperature, especially in the observation phase of the solar mode.

For the remaining tasks, the in-flight data from TSIM/FY-3A are known to suffer from solar pointing errors due to some data problems of the satellite. This is expected to be solved in the future. A preliminary analysis of the in-flight TSI data obtained with TSIM/FY-3B will be presented in an accompanying paper (Wang *et al.*, 2014). A complete reduction of the TSIM/FY-3B data incorporating the orbital position of the satellite requires a substantial development of analysis software and may take time.

Acknowledgements This work is supported by Development Plan Project for Science and Technology of Jilin Province (No. 20130101044JC) and Basic Research Project for application of Yunnan Province (No. 2012FD050). The authors would like to thank numerous staff in Changchun Institute of Optics, Fine Mechanics and Physics, Chinese Academy of Sciences, including Chenghu Gong, Dongjun Yang, Xin Ye, Jianbo Huang, and many others. The authors are grateful to Bingxi Yu, former project leader of the TSIM, for his great contributions and precious advice concerning the TSIM. The authors thank the referee for generous help and good comments.

References

Booth, M.: 2014, Adaptive optical microscopy – The ongoing quest for a perfect image. *Light Sci. Appl.* **3**, e165. DOI.

Fang, W., Yu, B., Yao, H., An, Y., Gong, C., Li, Z.: 2002, Development of STIM. In: Menzel, W.P., Zhang, W.J., Le Marshall, J., Tokuno, M. (eds.) *Applications with Weather Satellites*, *Proc. SPIE* **4895**, 218. DOI.

Fox, N., Kaiser-Weiss, A., Schmutz, W., Thome, K., Young, D., Wielicki, B., Winkler, R., Woolliams, E.: 2011, Accurate radiometry from space: An essential tool for climate studies. *Phil. Trans. Roy. Soc. A.* **369**, 4028. DOI.

Frohlich, C.: 2011, Total solar irradiance observations. *Surv. Geophys.* **32**, 1. DOI.

Frohlich, C., Andersen, N., Appourchaux, T., Berthomieu, G., Crommelynck, D., Domingo, V., Fichot, A., Finsterle, W., Gomez, M., Gough, D., Jimenez, A., Leifsen, T., Lombaerts Pap, J., Provost, J., Cortes, T., Romero, J., Roth, H., Sekii, T., Telljohann, U., Toutain, T., Wehrli, C.: 1997, First results from VIRGO, the experiment for helioseismology and solar irradiance monitoring on SOHO. *Solar Phys.* **170**, 1. DOI.

Girshovitz, P., Shaked, N.: 2014, Doubling the field of view in off-axis low-coherence interferometric imaging. *Light Sci. Appl.* **3**, e151. DOI.

Hoyt, D., Kyle, H., Hickey, J., Maschhoff, R.: 1992, The Nimbus 7 solar total irradiance: A new algorithm for its derivation. *J. Geophys. Res.* **97**, 51. DOI.

Kopp, G., Heuerman, K., Lawrence, G.: 2005, The Total Irradiance Monitor (TIM): Instrument calibration. *Solar Phys.* **230**, 111. DOI.
Kopp, G., Lawrence, G.: 2005, The Total Irradiance Monitor (TIM): Instrument design. *Solar Phys.* **230**, 91. DOI.
Liebetraut, P., Petsch, S., Liebeskind, J., Zappe, H.: 2013, Elastomeric lenses with tunable astigmatism. *Light Sci. Appl.* **2**, e98. DOI.
Mekaoui, S., Dewitte, S., Conscience, C., Chevalier, A.: 2010, Total solar irradiance absolute level from DIARAD/SOVIM on the international space station. *Adv. Space Res.* **45**, 1393. DOI.
Memarian, M., Eleftheriades, G.: 2013, Light concentration using hetero-junctions of anisotropic low permittivity metamaterials. *Light Sci. Appl.* **2**, e114. DOI.
Rubenchik, A., Fedoruk, M., Turitsyn, S.: 2014, The effect of self-focusing on laser space-debris cleaning. *Light Sci. Appl.* **3**, e159. DOI.
Wang, H., Li, H., Fang, W.: 2014, Timing parameter optimization for comparison experiments of TSIM. *Appl. Opt.* **53**, 1718. DOI.
Wang, H., Wang, Y.: 2012, Spaceborne radiometers for measuring total solar irradiance. *Chin. Opt.* **5**, 555. DOI.
Wang, H., Wang, Y., Fang, W.: 2011, Intelligent solar tracker with double modes. *Opt. Precision Eng.* **19**, 1605. DOI.
Wang, H., Li, H., Qi, J., Fang, W.: 2014, Total solar irradiance monitors for Chinese FY-3B satellite – space experiments and primary data corrections. *Solar Phys.*, accepted.
Wilson, R.: 1979, Active cavity radiometer type IV. *Appl. Opt.* **18**, 179. DOI.
Wilson, R.: 1997, Total solar irradiance trend during solar cycles 21 and 22. *Science* **277**, 1963. DOI.
Witte, S., Tenner, V., Noom, D., Eikema, K.: 2014, Lensless diffractive imaging with ultra-broadband table-top sources: From infrared to extreme-ultraviolet wavelengths. *Light Sci. Appl.* **3**, e163. DOI.
Yang, Z., Lu, N., Shi, J., Zhang, P., Dong, C., Yang, J.: 2012, Overview of FY-3 payload and ground application system. *IEEE Trans. Geosci. Remote Sens.* **50**, 4846. DOI.